10.1109/ULTSYM.2012.0349

# Simultaneous Photoacoustic Detection of Red Blood Cell Aggregation and Oxygenation

Eno Hysi, Ratan K. Saha and Michael C. Kolios

***Abstract*—Red blood cell (RBC) aggregation is a reversible process which occurs in the presence of increased plasma fibrinogen concentration and low flow conditions. It results in the RBCs forming structures that resemble "stacks of coins" and/or clusters impairing blood flow and the ability of oxygen to diffuse to surrounding tissues. We investigate the use of photoacoustics (PA) to detect and monitor RBC aggregation and the effect of aggregation on the sample oxygenation level. In this study, porcine RBCs were illuminated at 750nm and 1064 nm and the oxygen saturation of each sample was estimated. Aggregation was induced by varying the concentration of Dextran-70. Changes in the photoacoustic signal strength suggest that in the presence of RBC aggregates, the release of oxygen into the surroundings is impaired. A 30% increase in oxygen saturation was measured based on changes in the PA signal when comparing the non-aggregated and aggregated blood samples. This work demonstrates that PA imaging has the potential to detect changes due to RBC aggregation and monitor oxygenation level.**

***Keywords*—Photoacoustics, Red Blood Cell Aggregation, Oxygen Saturation.**

## I. Introduction

THE aggregation of red blood cells (RBCs) is a reversible phenomenon during which individual cells align face-to-face and form structures commonly referred to as rouleux. Aggregation is a naturally occurring, reversible process dictated by the concentration of soluble plasma proteins (i.e. fibrinogen) and the properties of the RBCs themselves (i.e. cell age and surface charge density) [1].

It has been shown that RBC aggregation plays a significant role in blood rheology. In the event of decreased blood flow (ex. in atherosclerotic plaques), the shear forces created due to blood velocity gradients decrease, thus enhancing aggregate formation [2]. This leads to increased viscosity at low shear rates. Significant enhancements in blood viscosity have been reported in the presence of aggregation developed in the myocardial circulation of patients with acute coronary syndromes [3]. In addition, aggregation contributes to an enhanced thickness of the plasma layer around blood vessels. This leads to a significant reduction in the diffusion of oxygen to the surrounding tissues [4], [5].

Both the aggregation of RBCs and the oxygenation of blood are important markers for making clinical decisions. Specifically, RBC aggregation is increased during acute phase reactions in response to infections, tissue injuries or immunological disorders [6]. Tissue oxygenation monitoring is important in managing a number of clinical situations such as during trauma or surgical interventions where oxygenation levels fluctuate [7].

Our group has reported on a theoretical model for the detection of RBC aggregation using photoacoustics (PA) [8] and more recently on the experimental detection of RBC aggregation [9]. In addition, we have developed the theoretical framework for investigating the effect of oxygenation of RBC samples on the PA signals and their respective power spectra [10], [11]. In this paper, we examine the simultaneous detection of RBC aggregation and oxygenation level using PA. The goal of this work is to develop a non-invasive assessment of RBC aggregation and its effect on the oxygenation level of RBCs.

## II. Materials and Methods

### A. Cell Preparations

Fresh porcine blood from the femoral vein of Yorshire pigs (Comparative Research, Toronto, ON) was drawn into $K_2$-EDTA vacutaners (Becton, Dickinson and Company, Franklin Lakes, NJ). The RBCs were isolated by centrifugation (1500 g, 6 minutes, 25°C). The packed RBCs were washed with phosphate buffered saline (PBS) twice and were re-suspended in PBS in order to achieve 3 hematocrit levels (10%, 20% and 40%). For each hematocrit level, aggregation was induced by suspending the RBCs in varying concentrations of Dextran-70 (Sigma-Aldrich, St. Louis, MO) dissolved in PBS. By changing the Dextran-70-PBS concentration ([Dex]), varying degrees of aggregation were achieved. For this study, the [Dex] were 1%, 3% and 8% (wt/vol). The presence of aggregation was assessed by optical inspection of the blood samples using an Olympus CKX41 optical microscope (Olympus Canada Inc., Markham, ON).

### B. PA Setup

The PA measurements of all samples used in this study were

E. Hysi was with Department of Physics, Ryerson University, Toronto, ON., Canada. He is now at the Louisiana State University School of Medicine MD-PhD Program, New Orleans, LA., USA (e-mail: ehysi@lsuhsc.edu).

R. K. Saha is with the Applied Material Science Division, Saha Institute of Nuclear Physics, Kolkata, India (e-mail: ratank.saha@saha.ac.in).

M. C. Kolios is with the Department of Physics, Ryerson University, Toronto, ON., Canada (e-mail: mkolios@ryerson.ca).

conducted using the Imagio Small Animal PA Imaging Device (Seno Medical Instruments Inc., San Antonio, TX) shown in Fig. 1.

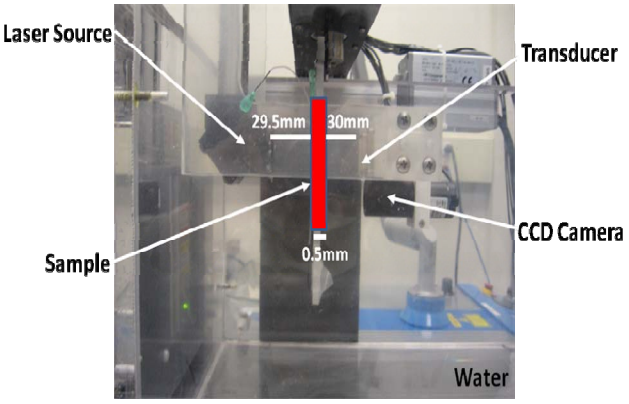


Fig. 1. Photograph of the PA setup.

The system consisted of a Q-switched, pulsed Nd:YAG laser delivered through an articulated arm and a transducer located 60 mm coaxial to the laser that was raster scanned. Each sample was irradiated at 750 nm and 1064 nm (9 mm beam diameter, 6 ns pulse width, 10 Hz pulse repetition rate, 25 mJ/cm$^2$ energy fluence per pulse). The transducer used to record the PA signals consisted of 4 elements arranged in an annular array (5 MHz center frequency, 60% -6dB bandwidth).

Each RBC sample (non-aggregated and aggregated) was loaded into cylindrical tubes and placed at the focus of the ultrasonic transducer (29.5 mm). In order to expose the entire suspension inside the tube, a vertical raster scan was performed. For each scan, the laser emitted 4 pulses at each location and the PA signals produced from each pulse were averaged to generate 1 PA radio-frequency (RF) signal. A total of 80 laser pulses were fired at each sample corresponding to 20 RF signals at different locations inside the tube (0.5 mm apart, 10 cm total length).

### C. Data Analysis

For each PA signal recorded, the PA signal strength (PSS) was computed as the integration of the Hilbert Transform of the PA signal. The average PSS along with the standard deviation was calculated for each exposed solution at each hematocrit and [Dex]. The normality of the data was confirmed using a Shapiro-Wilk test (normality criterion W > 0.05). An unpaired t-test was used to compare the PSS from non-aggregated and aggregated RBCs. Statistical significance was established for p-values of 0.05 or less.

### D. Oxygen Saturation Estimation

The oxygen saturation ($SO_2$) of each sample was estimated by illuminating at both wavelengths (750 nm and 1064 nm) and taking into account the fact that the PSS is directly proportional to the concentration of oxygenated and deoxygenated hemoglobin, OHb and DHb, respectively [12]. Assuming that OHb and DHb are the dominant absorbers at each wavelength of illumination, the $SO_2$ can be estimated by

$$SO_2 = \frac{[OHb]}{[OHb]+[DHb]} = \frac{PSS(\lambda_2)\times\varepsilon(DHb,\lambda_1) - PSS(\lambda_1)\times\varepsilon(DHb,\lambda_2)}{PSS(\lambda_1)\times\Delta\varepsilon(\lambda_2) - PSS(\lambda_2)\times\Delta\varepsilon(\lambda_1)} \quad (1)$$

Here, $\Delta\varepsilon(\lambda) = \varepsilon(OHb,\lambda) - \varepsilon(DHb,\lambda)$ is the difference in extinction coefficient $\varepsilon$ for each wavelength of illumination $\lambda$. In this study, $\lambda_1 = 750$ nm and $\lambda_2 = 1064$ nm .

## III. Results and Discussion

The experimentally measured PSS for all samples are shown in Fig. 2. Fig. 2(a) contains the PSS for the 750 nm exposure. The PSS for the 1064 nm exposure are shown in Fig. 2(b). The PSS is plotted as a function of both the hematocrit (10%, 20% and 40%) and [Dex] (i.e. aggregation level). For both wavelengths of illumination, the PSS increased monotonically with increasing hematocrit. The increase was ~1.3x per doubling hematocrit level. As we have previously reported [8-12], the monotonic increase in PSS with increasing hematocrit is due to the increase in the concentration of optical absorbers (i.e. the RBCs). This relationship enables the estimation of the hematocrit level using the PSS. The hematocrit level is a parameter that is used in making clinical decisions [1]. Furthermore, it provides an improvement over other non-invasive means of estimating hematocrit in the presence of aggregates such as ultrasound imaging where the relationship between the backscattered signals and hematocrit is relatively complex [13].

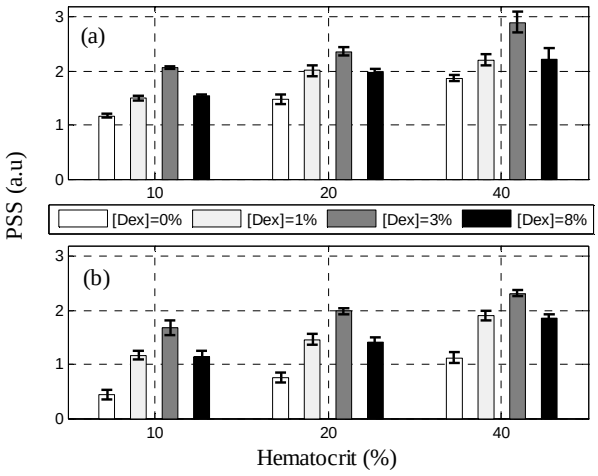


Fig. 2. Experimentally measured PSS for all RBC samples irradiated at (a) 750 nm and (b) 1064 nm at three different hematocrit levels and four different aggregation levels. The error bars denote the standard deviations of 20 PA signals.

As the aggregation level was varied, the PSS exhibited a non-linear trend. The maximum PSS was achieved for a [Dex] of 3% at all hematocrit levels. The 1% and 8% [Dex] exhibited nearly identical PSS (p = 0.2). The PSS for non-aggregated samples ([Dex] = 0%) was at least 1.6x smaller than the aggregated samples at all hematocrit levels, for both wavelengths of illumination (p = 0.001). These trends in PSS

correlate well with other independent assessments of RBC aggregation for these [Dex] [14], [15]. The 3% [Dex] results in the formation of the largest aggregates thus providing the largest increase in the PSS compared to the non-aggregated sample. Our theoretical model suggests that when the RBCs form aggregates, significant changes in the PA signals occur, consistent with the aggregates acting as a larger PA source [8], [9]. In addition, for the 750 nm exposure, the PSS was ~1.3x greater than the 1064 nm exposure for all samples measured ($p = 0.003$). Since the RBCs were kept at the same environmental conditions, the change in PSS could be attributed to the oxygen-dependent optical absorption of the RBCs [16].

Fig. 3 shows the $SO_2$ calculated by utilizing (1) with both exposure wavelengths. The $SO_2$ increased linearly with increasing hematocrit with an average increase of ~7% per doubling hematocrit level. At the 3% [Dex], $SO_2$ was at the highest level, specifically 30% higher than the non-aggregated case ($p = 0.00001$). The 1% and 3% [Dex] $SO_2$ levels were virtually identical at all hematocrit levels and ~20% higher than the non-aggregated samples ($p = 0.00003$). It appears that the presence of aggregation increases the $SO_2$ level. This suggests that aggregation decreases the ability of RBCs to release oxygen to the surrounding environment. Such an observation has important implications for oxygen transfer from the RBCs to the surrounding tissues. The impaired oxygen diffusion in the presence of aggregation has been attributed to an increase in the thickness of the aggregant layer engulfing the aggregates [17]. Similar increases in the $SO_2$ level with aggregation have been measured experimentally using a microscope system coupled with a spectrophotometer [5]. The ability of PA to detect the increase in $SO_2$ with increasing aggregation level suggests that it might be possible to simultaneously detect the presence of aggregation and assess the oxygenation level of the same sample. This could potentially allow for a means of making an assessment of the impact of RBC aggregation on tissue oxygenation levels.

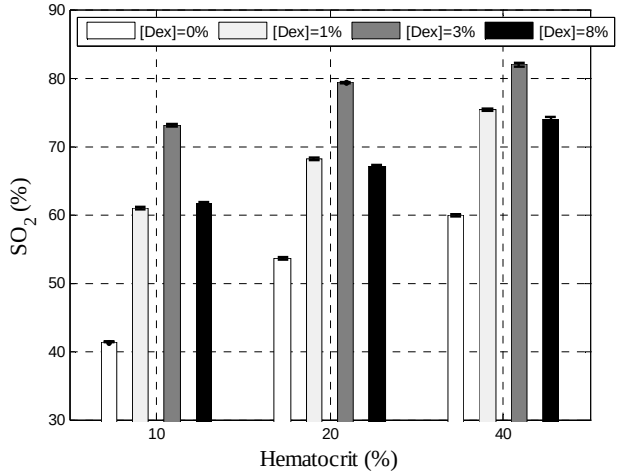


Fig. 3. Calculated $SO_2$ for all RBC samples at three different hematocrit levels and four different aggregation levels. The error bars denote the standard deviation of 20 PA signals.

## IV. Conclusion

This papers reports on the effect of RBC aggregation on the oxygenation level of the sample as detected non-invasively using photoacoustics. The results of this work suggest that RBC aggregation significantly increases the oxygen saturation of the blood sample, thus potentially affecting the release of oxygen in the surrounding tissue in-vivo.

## Acknowledgement

This work was made possible due to the financial support of the following granting agencies awarded to M. C. Kolios: Natural Sciences and Engineering Research Council of Canada, Canadian Institutes of Health Research, Canadian Foundation for Innovation, Canada Research Chairs Program and the Terry Fox Foundation. E. Hysi was supported through the Alexander Graham Bell Graduate Scholarship. The authors would like to thank A. Worthington and J. Barry for their assistance during this project.

## References

[1] O. K. Baskurt, B. Neu and H. J. Meiselman, *Red Blood Cell Aggregation*. Boca Raton, FL: CRC Press, 2011, pp. 1-304.

[2] B. Neu and H. J. Meiselman, "Red blood cell aggregation," in *Handbook of Hemorheology and Hemodynamics*, O. K. Baskurt, M. R. Hardeman, M. W. Rampling, and H. J. Meiselman, Eds. Amsterdam: IOS Press, 2007, pp. 114-136.

[3] Y. Arbel et al., "Erythrocyte aggregation as a cause of slow flow in patients of acute coronary syndromes," *Int. J. Cardiol,*. vol. 154, pp. 322-327, 2012.

[4] N. Tateishi, Y. Suzuki, M. Shirai, I. Chicha and N. Maeda, "Reduced oxygen release from erythrocytes by the acceleration-induced flow shift, observed in an oxygen-permeable narrow tube," *J. Biochem,*. vol. 35, pp. 1241-1251 , 2002.

[5] N. Tateishi, N. Maeda and T. Shiga, "A method for measuring the rate of oxygen release from single microvessels," *Circ. Res.*, vol. 70, pp. 812-819, 1992.

[6] X. D. Weng, G. Cloutier, R. Beaulieu and G. O. Roederr, "Influence of acute-phase proteins on erythrocyte aggregation," *Am. J. Physiol. Heart Circ. Physiol.*, vol. 271, pp. H2346-H2352, 1996.

[7] H. F. Zhang, K. Maslov, M. Sivaramakrishnan, G. Stoica and L. V. Wang, "Imaging of the hemoglobin saturation variation in single vessels in vivo using photoacoustic microscopy," *App. Opt.*, vol. 90, pp. 053901, 2007.

[8] R. K. Saha and M. C. Kolios, "A simulation study on photoacoustic signals from red blood cells," *J. Acoust. Soc. Am.*, vol. 129, no. 4, pp. 2935-2943, 2011.

[9] E. Hysi, R. K. Saha and M. C. Kolios, "On the use of photoacoustics to detect red blood cell aggregation," *Biomed. Opt. Express*, vol. 3, no. 9, pp. 2326-2338, 2012.

[10] R. K. Saha and M. C. Kolios, "Effects of erythrocyte oxygenation on optoacoustic signals," *J. Biomed. Opt.*, vol. 16, pp. 115003, 2011.

[11] R. K. Saha, S. Karmakar, E. Hysi, M. Roy and M. C. Kolios, "Validity of a theoretical model to examine blood oxygenation dependent photoacoustics," *J. Biomed. Opt.*, vol. 17, no. 5, pp. 055002, 2012.

[12] X. Wang, X. Xie, G. Ku, L. V. Wang and G. Stoica, "Noninvasive imaging of hemoglobin concentration and oxygenation in the rat brain using high-resolution photoacoustic tomography," *J. Biomed. Opt.*, vol. 11, no. 2, pp. 024015, 2006.

[13] F. T. Yu and G. Cloutier, "Experimental ultrasound characterization of red blood cell aggregation using the structure factor size estimator," *J. Acoust. Soc. Am.*, vol. 122, no. 1, pp. 645-656, 2007.

[14] O. K. Baskurt, R. A. Farley and H. J. Meiselman, "Erythrocyte aggregation tendency and cellular properties in horse, human and rat: a

comparative study," *Am. J. Heart Circ. Physiol.*, vol. 273, pp. H2604-H2612, 1997.
[15] O. K. Baskurt and H. J. Meiselman, "Blood rheology and hemodynamics," *Semin. Thromb. Hemost.*, vol. 29, no. 5, pp. 435-450, 2003.
[16] L. V. Wang, "Prospects of photoacoustic tomography," *Med. Phys.*, vol. 35, no. 12, pp. 5758-5776, 2008.
[17] N. Tateishi, N. Maeda and T. Shiga, "Flow dynamics of erythrocytes in microvessels of isolated rabbit mesentery: cell-free layer and flow resistance," *J. Biochem.*, vol. 27, no. 9, pp. 1119-1125, 1994.